From laser-scanned data to feature human model: a system based on fuzzy logic concept

Charlie C.L.Wang[*]   **Terry K.K.Chang**   **Matthew M.F.Yuen**

Department of Mechanical Engineering, Hong Kong University of Science and Technology,

Clear Water Bay, Kowloon, Hong Kong

Abstract

This paper describes the development of a prototype system using fuzzy logic concept for constructing a feature human model, which is to be stored in a 3D digital human model database. In our approach, the feature human model is constructed by unorganized cloud points obtained from 3D laser scanners. Firstly, noisy points are removed, and the orientation of the human model is adjusted; secondly, a feature based mesh generation algorithm is applied on the cloud points to construct the mesh surface of the human model; lastly, semantic features of the human model are extracted from the mesh surface. Compared with earlier approach, our method strongly preserves the topology of a human model; more details can be constructed; and both the robustness and the efficiency of the algorithm are improved. At the end of the paper, in order to demonstrate the functionality of feature human models, potential applications are given.

Keywords: feature recognition, reverse engineering, fuzzy logic, fashion industry, computer aided engineering.

1. Introduction

The work presented in this paper comes from the project of building a 3D digital human model database, which is important to help an apparel enterprise to stay ahead of current technology innovations promoted by major retailers and manufacturers. Reverse engineering (RE) plays a prominent role in computer aided engineering (CAE) systems. In RE systems, the geometric model of an object is generated from a cloud of points, which can be obtained by three main techniques [1]: 1) coordinate measuring machines (CMMs); 2) 3D laser scanners; and 3) digital photogrammetry systems. The laser scanner is the most common solution because it is fast and robust relative to other methods. Moreover, scanned data from a laser provides the explicit 3D

---

[*] Corresponding Author: Charlie C. L. Wang; E-mail: wangcl@ust.hk; Tel: (852) 2358-8095; Fax: (852) 2335-9298

points position from which a 3D model can be reconstructed [2]. Thus, the cloud points for constructing a feature human model are to be obtained from 3D laser scanners in our approach.

The features extracted from the human model are the major contribution of the database to the fashion industry. In the features modeling field, object semantics are systematically represented for a specific application domain; in other words, a semantic feature is an application-oriented feature defined on geometric elements. There are two approaches for building a feature model [3]: 1) The design by feature approach creates the feature model of an object by composing the available features in a feature library; 2) The feature recognition approach recognizes various feature from a geometric model of an object according to the feature templates defined in a feature library. This paper describes an approach of constructing feature human models from unorganized cloud points according to the feature templates using fuzzy logic. A facet model with features defined is the final model stored in the 3D digital human model database.

The target sample data size of the digital human model database is more than 2000 persons. Thus, the robustness and efficiency of the system is very important; and to provide conveniences to the downstream applications, the topology of each human model should be strongly preserved. The whole procedure of the system consists of three steps: 1) data preparation – filter noise and adjust orientation; 2) human model construction – construct the mesh model of a human; 3) semantic feature extraction – extract the semantic features from the mesh surface of a human model (The flow chart is shown in Fig. 1).
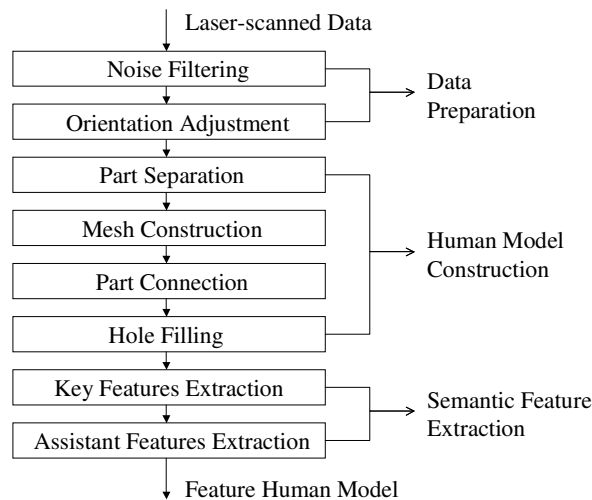

Fig. 1 System flow chart

2. Literature Review

There is a large quantity of work related with building the geometric model of an object from a cloud of points. Hoppe et al. [4] presented a general method for automatic reconstruction of accurate, concise, piecewise

smooth surface models from scattered range data. However, in their method, it is hard to preserve the topology of the constructed geometry model; and their algorithm is very time-consuming. Ko et al. [5] proposed a method to model a human face from a set of points. Their discussion concentrated on the re-organization of the points, facet modeling and tool path generation. Ma and He [6] presented an approach to shape a single B-spline surface with a cloud of points. Their approach mainly focuses on the parameterization of the unorganized points. Barhak and Fischer [7] also presented a PDE based method about the parameterization for reconstruction of 3D freeform objects from laser-scanned data. Sienz et al. [8] developed a fitting technique to generate computational geometric models of 3D objects defined in the form of a point cloud. Doncesu [9] meshed the surface a object from a cloud of points using the Delaunay triangulation. Rodriguez et al. [10] developed another Delaunay triangulation based surface reconstruction algorithm. All the above approaches are geometry oriented and feature technology does not benefit the mesh construction process. In order to create a feature model of an object from a point cloud, the embedded features must be recognized; and the features also benefit the surface construction process.

Dobson et al. [11] discussed the fitting of a non-uniform rational B-spline curve to a set of co-planar points. The whole process is based on fitting characteristic points by optimizing vertices and weights of a rational B-spline curve. Their feature based modeling approach is demonstrated in 2D by the fitting of facial profiles. Au and Yuen [3] discussed the issues of applying feature technology to the reverse engineering of a mannequin. In their approach, the feature model of a mannequin consists of the major features of the torso for garment design, and the features are recognized from the point cloud by comparing it with a generic feature model. Association is set up between the point cloud and the mannequin features. Fitting the generic feature model to the point cloud yields the mannequin feature model of a specific person. This is achieved by optimizing the distance between the point cloud and the feature surface, subject to the continuity requirements. However, the task of matching the critical points is done manually in their approach. Since surface fitting forms the shape of the human model, it is hard to capture details; and the process of surface fitting is very time consuming.

This paper presents a feature based approach of building a human model from a point cloud. Firstly, noisy points are removed, and the orientation of the human model is adjusted; secondly, a feature based mesh generation algorithm is applied on the cloud points to construct the mesh surface of the human model; lastly, semantic features of the human model are extracted from the mesh surface. The whole system is based on fuzzy logic concept. Compared with earlier methods, the advantages of our approach are: 1) the topology of a human

model is strongly preserved; 2) more details can be constructed; 3) the robustness is improved; and 4) the algorithm is more efficient.

3. Notations and Definitions

Before we describe the whole system, some definitions of the notations are given as follows. The total number of points of the scanned human model Ω is defined by N_P; $X(P_i)$, $Y(P_i)$, and $Z(P_i)$ represent the X, Y, and Z coordinate of points P_i in Ω; $X_{\max}(S)$, $Y_{\max}(S)$, and $Z_{\max}(S)$ represent the maximum X, Y, and Z coordinate of a set of points – S, and $X_{\min}(S)$, $Y_{\min}(S)$, and $Z_{\min}(S)$ represent the minimum X, Y, and Z coordinate of S; $\wedge S$ represents the back part of point set S, and $\vee S$ represents the front part of point set S (the "front" and "back" correspond to the x-axis). The mesh surface of the human model Ω is represented by Ω_M.

In our system, the orientation of the coordinate system is defined as follows: the x-axis is pointing out of the screen, the y-axis is horizontally pointing to the right in the screen plane, and the z-axis is vertically pointing upwards in the screen plane.

4. Data Preparation

Since the point cloud obtained from 3D laser scanners always has some noisy points, and its orientation sometimes does not face the x direction (Fig. 2a), we have to modify the point cloud to make it ready for mesh construction.
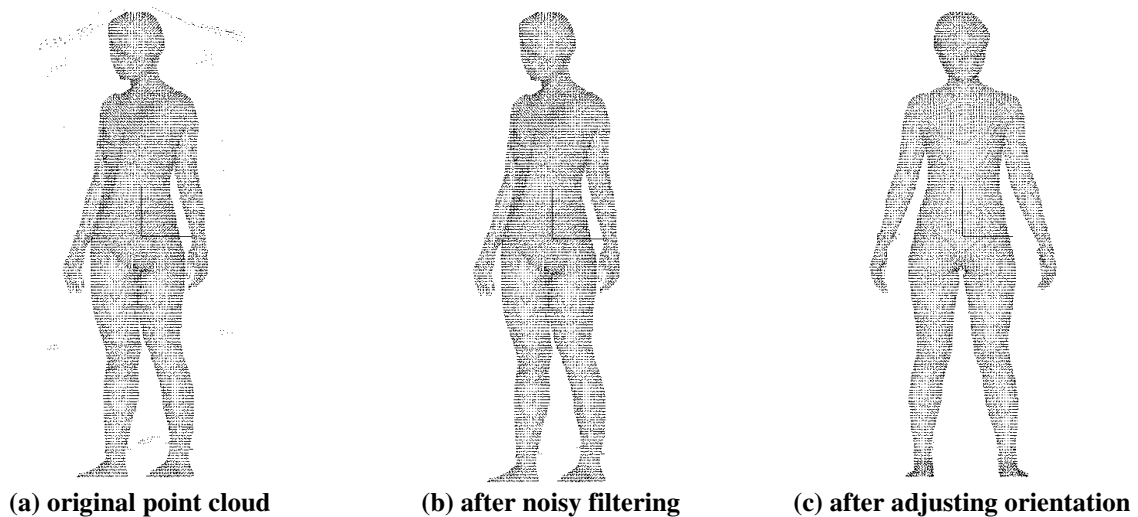

(a) original point cloud   (b) after noisy filtering   (c) after adjusting orientation

Fig. 2　Data preparation

4.1 Noise Filtering

After observing the output point cloud of the 3D laser scanner, it is not hard to find that the noisy points always have a "far" distance from the surface of the human model. When a person is asked to manually delete the noisy points, his intention is to delete the points "far" from the human model. There are a lot of filtering techniques in the binary digital image-processing field [12]; most of them are based on the definition of neighborhood by a discrete distance function. However, when applying these techniques on the 3D point cloud, it is extremely hard to choose a distance function since the neighborhood relationship can be evaluated vaguely in our case. Therefore, a filtering system needs to be capable of reasoning with vague and uncertain information; this suggests the use of fuzzy logic.

It is very important to select membership functions that can reflect this intention correctly and precisely. Another criterion for selecting membership function is computational efficiency [13]. Thus, we choose a triangular membership function (shown in Fig. 3). The membership function considered here is the distance between two points. The function is defined as follows:

$$\mu_{DistanceSmall}(x) = \begin{cases} \dfrac{DistanceAve - x}{DistanceAve - DistanceMin} & DistanceMin < x \le DistanceAve \\ 1 & x \le DistanceMin \\ 0 & otherwise \end{cases} \quad (1)$$

$$\mu_{DistanceNormal}(x) = \begin{cases} \dfrac{x - DistanceAve}{DistanceAve - DistanceMin} & DistanceMin < x \le DistanceAve \\ \dfrac{DistanceMax - x}{DistanceMax - DistanceAve} & DistanceAve < x < DistanceMax \\ 0 & otherwise \end{cases} \quad (2)$$

$$\mu_{DistanceLarge}(x) = \begin{cases} \dfrac{x - DistanceAve}{DistanceMax - DistanceAve} & DistanceAve < x \le DistanceMax \\ 1 & x > DistanceMax \\ 0 & otherwise \end{cases} \quad (3)$$
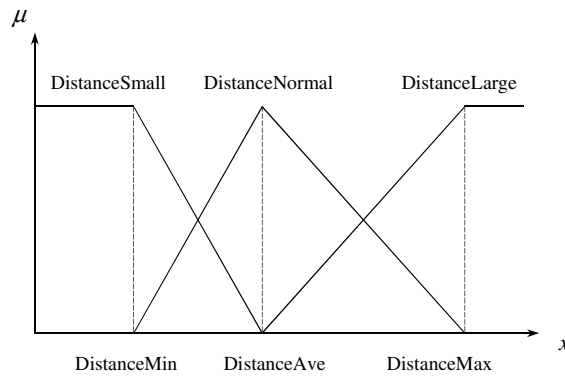

Fig. 3 Membership function of distance between two points

Our fuzzy filter uses fuzzy inference rules to preprocess the point cloud in order to delete noisy points. Capturing a person's intention of filtering noise, we define the following rules to identify noisy points:

Rule 1: When consider two points, if the distance between them is "large", they should belong to different sets; otherwise, they belong to the same set.

Rule 2: After clustering all points, the set with maximum points number is the set containing the points of the human model; the other sets are the sets of noisy points.

After applying the rule 1 on the point cloud from the 3D laser scanner, the points are separated into several sets. Containing the point set of the human model and deleting the noisy point sets according to the rule 2, we obtain the filtering result (as shown in Fig. 2b).

4.2 Orientation Adjustment

In our scanner settings, the facing direction of the scanned individual is free. Thus, the orientation of the scanned data is not uniform, which will cause troubles in the following feature extraction steps. We should adjust the orientation of the individuals to make them face the x-axis in the model space (as shown in Fig. 2c).
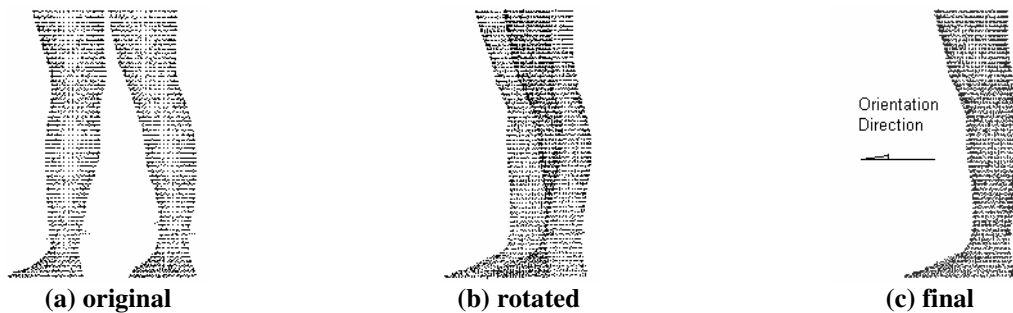

| (a) original | (b) rotated | (c) final |

Fig. 4   Adjust orientation of the human model

When we want to find the orientation of a human model, we always rotate it and observe its legs (see Fig. 4). If its two legs are totally overlapped, we can conclude that the orientation of the human model is facing left or facing right. Then if the toe tips of the human model are facing left, the orientation of the human model is facing left; and if the toe tips of the human model are facing right, its orientation is facing right. That is the knowledge of how to detect the orientation. Our system expresses this detecting method in knowledge rules and integrates them into a program by condition statements (*if-then*). But while writing above knowledge into condition statements, we find that it is difficult to expressed. It must be converted into a form that is easy to be implemented in a computer system. We find that when the two legs are overlapped, the width of the projected points at the knee is the smallest in all cases; and when the width is the smallest, the two legs are overlapped. Thus, the condition of the projected points' width at the knee is applied to replace the overlap condition; and we simply use the 1/4 height of a human model as its knee place. The rule is:

if

- The width, $W(S_k)$, of the set of projected points, S_k, is the smallest while rotating the human model along the vertical axis, where $S_k = \{P_i \mid Z_{\min}(\Omega) + \frac{1}{4}h_b - \varepsilon < Z(P_i) < Z_{\min}(\Omega) + \frac{1}{4}h_b + \varepsilon, P_i \in \Omega\}$, $W(S_k) = Y_{\max}(S_k) - Y_{\min}(S_k)$, h_b is the height of the human model, and ε is a very small number (e.g., 2mm).

then

- The orientation of the human model is to the left or right.

Now the only left thing is to detect whether the toe tips of the human model is facing left or facing right. By observing Fig. 4c, we find that the horizontal distance from the toe tips to the ankle is larger than the horizontal distance from the heel to the ankle. Using this feature, we can determine whether the human model is facing left or facing right. The knowledge is represented by the following *if-then* rule:

if

- $Y_{\min}(S_a) - Y_{\min}(S_b) > Y_{\max}(S_b) - Y_{\max}(S_a)$, where

  $S_b = \{P_i \mid Z_{\min}(\Omega) < Z(P_i) < Z_{\min}(\Omega) + \varepsilon, P_i \in \Omega\}$ (the points set at the bottom of the human model),

  $S_a = \{P_i \mid Z_{\min}(\Omega) + \frac{1}{20}h_b - \varepsilon < Z(P_i) < Z_{\min}(\Omega) + \frac{1}{20}h_b + \varepsilon, P_i \in \Omega\}$ (the points set of the ankle cutting plane), and ε is a very small number (e.g., 2mm).

then

- The orientation of the human model is to the left.

else

- The orientation of the human model is to the right.

In this rule, we use the position at the 1/20 height of a human model as its ankle place.

After detecting the orientation of the human model Ω, we rotate Ω to make it facing along the x-axis in the model space.

5. Human Model Construction

Nowadays polygonal meshes are widely used as a fundamental representation for geometric modeling in general. Thus, we represent human models by polygonal meshes in our database. After the noise of the point cloud is filtered and the orientation is adjusted, we assume that every remaining point is on the surface of the human model. The whole procedure of the mesh human construction consists of four steps: 1) separate the

whole point cloud into several parts (Fig. 5a and 5b); 2) construct the mesh surface of each part (Fig. 5c); 3) connect the mesh surfaces to build the whole human model (Fig. 5d); and 4) fill the holes (Fig. 5e). The details of each step are described below.
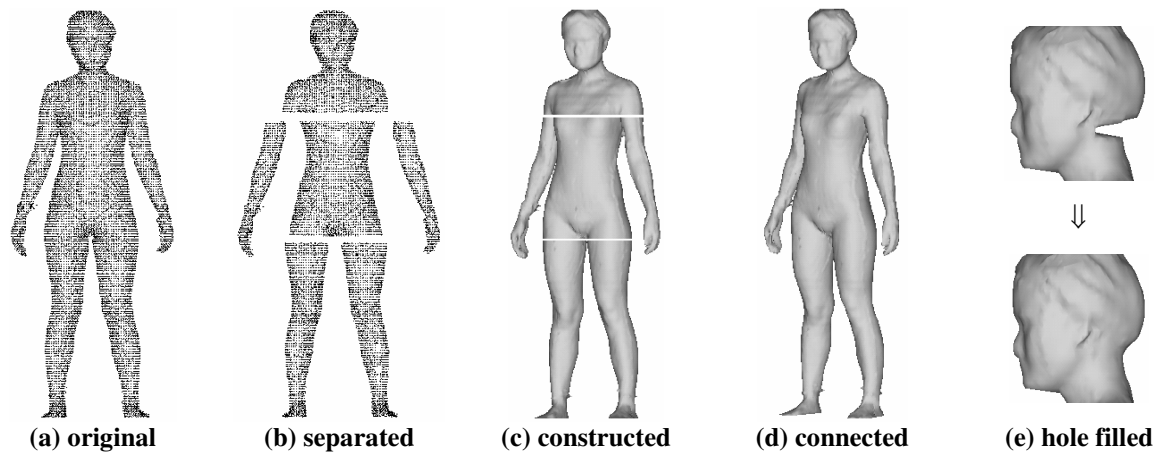

(a) original　　**(b) separated**　　**(c) constructed**　　**(d) connected**　　**(e) hole filled**

Fig. 5　Human model construction

5.1 Part Separation

In our system, the whole human body is separated into six parts (the structure of the six parts is shown in Fig. 6): the head root, the major body, the left arm, the right arm, the left leg and the right leg. The major body, the left arm, and the right arm are connected to the head root at the armhole; and the left and right legs are connected the major body at the crotch (Fig. 7). The armhole and the crotch are the two key features for separating the parts. Part separation is very straightforward after finding these key features. Thus, the most important issue in this section is how to extract these two key features from the point cloud.
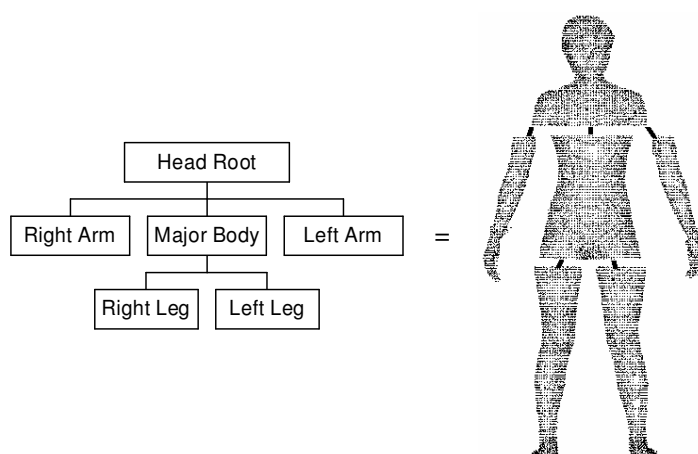

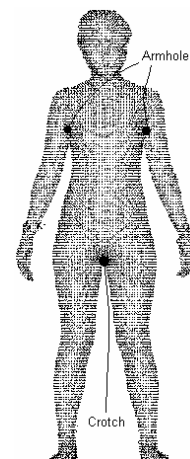
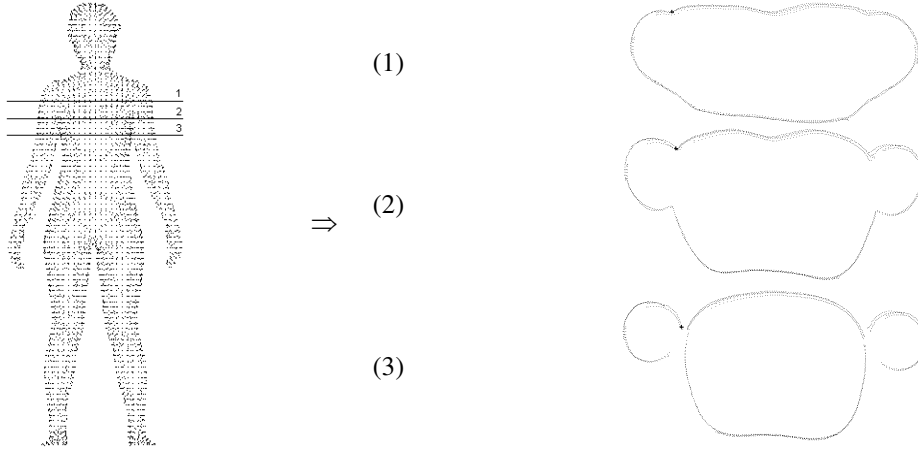**Fig. 6　Structure of human parts**　　　　**Fig. 7　Key features**

8

Fig. 8　Find armhole

In our approach, we extract the two key features by using horizontal cutting planes. From the intersection shapes of the three horizontal cutting planes in Fig. 8., we find that the armhole feature points are determined once we have identified a horizontal cutting plane with turning points. We search such a horizontal cutting plane from the top of the human model downwards. Fig. 9 shows the turning points of a horizontal cutting plane. If the angle on one point is "sharp", the point is a turning point. Here, we use the following methods to approximate the angle of point P_i (where $P_i \in S_p$, S_p is the set of points on a horizontal cutting plane p).

if

- $P_i \in \wedge S_p$, P_l is the left neighboring point of P_i on $\wedge S_p$, and P_r is the right neighboring point of P_i on $\wedge S_p$, where $\wedge S_p$ represents the back part of S_p, $|Y(P_i) - Y(P_l)| = \delta$, $|Y(P_i) - Y(P_r)| = \delta$, and δ is a very small number (e.g., 5mm).

then

- the angle of point P_i is $\angle P_l P_i P_r$.

or

if

- $P_i \in \vee S_p$, P_l is the left neighboring point of P_i on $\vee S_p$, and P_r is the right neighboring point of P_i on $\vee S_p$, where $\vee S_p$ represents the front part of S_p, $|Y(P_i) - Y(P_l)| = \delta$, $|Y(P_i) - Y(P_r)| = \delta$, and δ is a very small number (e.g., 5mm).

then

- the angle of point P_i is $\angle P_l P_i P_r$.

The following fuzzy rule is used to determine the position of the turning points.

9

Rule 3: The point with its angle "small" is a turning point.

The membership function of AngleSmall, AngleNormal, and AngleLarge is shown in Fig. 10. After finding the four turning points on a horizontal cutting plane (Fig. 9), the armhole feature is determined.
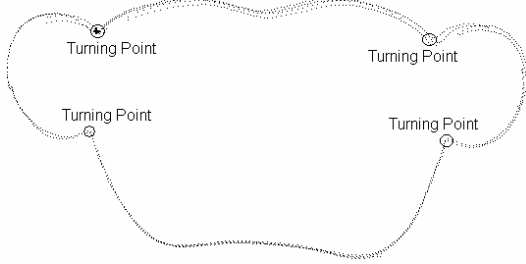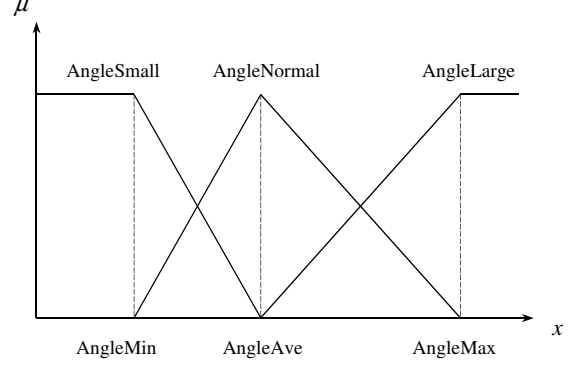

Fig. 9   Turning points

Fig. 10   Membership function of AngleSmall, AngleNormal, and AngleLarge

From the intersection shape of the three horizontal cutting planes in Fig. 11., we can define the following method to determine the position of the crotch feature: cutting the human body from its 1/2 height downwards, once the intersection breaks up into two circles, the crotch feature lies on a line in the gap equidistant from both of them. Here, we use the following method to determine whether the intersection breaks up into two circles (where $P_i \in S_p$, S_p is the set of points on a horizontal cutting plane p, and $\frac{7}{8}h_b$ is the approximate position of the neck).

if

- $S_g = \phi$, where $S_g = \{P_i \mid Y_c - w < Y(P_i) < Y_c + w, P_i \in S_p\}$, $Y_c = (Y_{\max}(S_c) + Y_{\min}(S_c))/2$,

  $S_c = \{P_i \mid Z_{\min}(\Omega) + \frac{7}{8}h_b - \varepsilon < Z(P_i) < Z_{\min}(\Omega) + \frac{7}{8}h_b + \varepsilon, P_i \in \Omega\}$, h_b is the height of the human

  model, ε is a very small number (e.g., 2mm), and w is another small number (e.g., 5mm).

then

- the major part of S_p breaks into two circles.

As mentioned above, after finding the plane in which the major part of the intersection breaks into two circles, we can determine the position of the crotch feature that lies on a line in the gap equidistant from both of them.
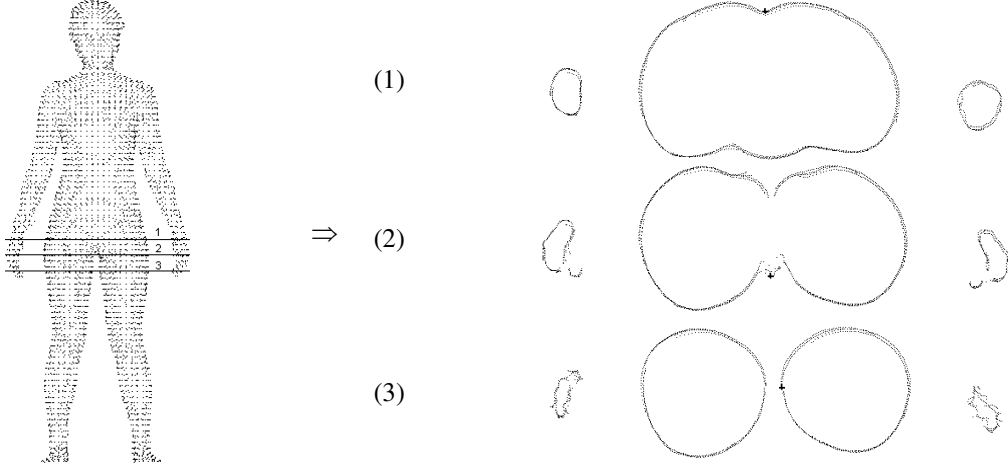
Fig. 11 Find crotch

5.2 Mesh Construction

After determining the position of the armhole feature and the crotch feature, it is easy to separate the point cloud of the human model into six parts (see Fig. 6). This is straightforward. In this section, we will describe how to construct the mesh surfaces of each part. The shape of each human part is "cylinder" like, so we develop a fast mesh generation algorithm depending on this characteristic. The procedure for mesh generation has two steps: 1) contour curve generation, and 2) surface construction from contours.

Contour curve generation: Since the whole human model is separated into six parts, the shape of the horizontal intersection of each part is similar to an ellipse. Here, we use polar decomposition method to approximate a polygonal curve C_p by the points on the horizontal cutting plane S_p. Firstly, the whole polar space is divided into N_θ intervals. Secondly, the polar coordinates of each point $P_i - (\theta(P_i), \rho(P_i))$ are determined (the center of the bounding box of points on S_p is used as the center of the polar coordinate system). Thirdly, N_θ subsets of S_p are determined by

$$S_p^i = \{P_i \mid \theta(P_i) \in \left[i\frac{2\pi}{N_\theta}, (i+1)\frac{2\pi}{N_\theta} \right), P_i \in S_p \} \tag{4}$$

where $i = 0, \ldots, N_\theta - 1$. Lastly, the mean point $\overline{P}(S_p^i)$ of points inside S_p^i is computed, and these points are connected in an ascending order of i to form the contour polygonal curve C_p of S_p. If $S_p^i = \phi$, that means there is a hole in the collected data of the human model from laser scanners; we use the polar coordinate $(i\frac{2\pi}{N_\theta}, \rho(\overline{P}(S_p^{i-1})))$ as the position of $\overline{P}(S_p^i)$; and a flag should be stored at $\overline{P}(S_p^i)$ for the following processes of filling holes. The contour curves generation result of each part is shown in Fig. 12
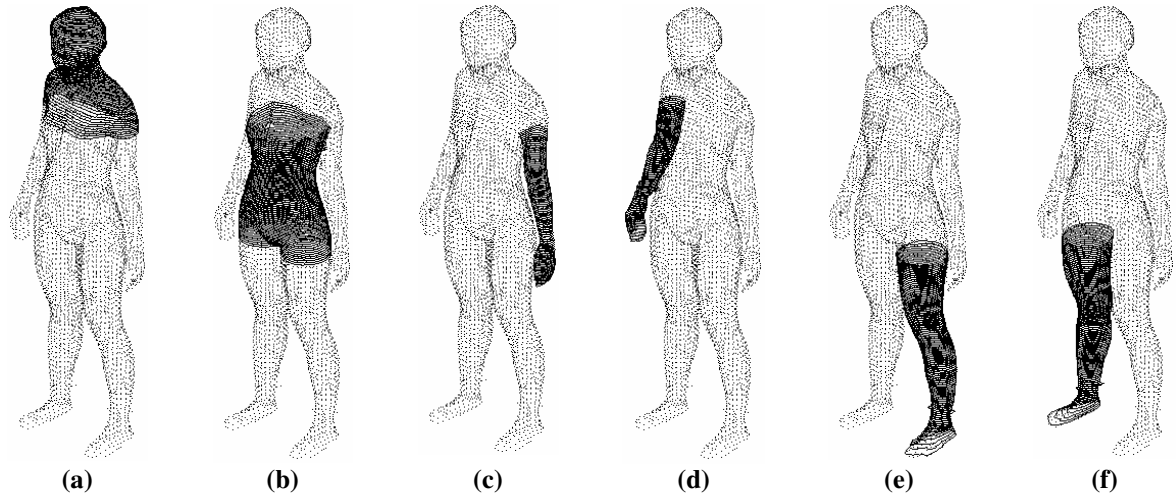
11

Fig. 12   Contour line generation result of each part

Surface construction from contours: In this mesh construction step, we create new polygons by sewing the neighboring copies of contour curves together [14, 15] (Fig. 13). After sewing the adjacent contour curves, new 3D polygonal surfaces of each part of the human model are created (Fig.14).
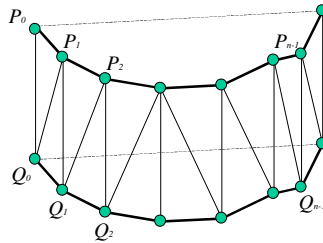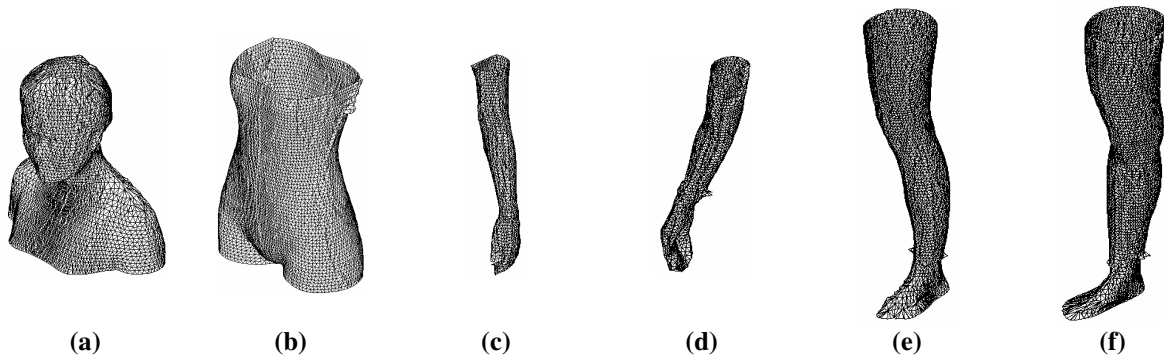

Fig. 13   Sew neighboring contours

Fig. 14   Mesh construction result of each part

5.3 Part Connection

After constructing the mesh surface of each human part, they must be connected by some new triangles to generate a continuous mesh surface. Here, we use the approach of Ekoule et al. [16] to solve this problem. In their approach, when two adjacent slides contain a different number of contours (e.g., one slide contains only one contour, but another slide contains more than one contours), a new and unique interpolated contour is

generated between the two slides, and the link is created by using this new constructed contour. The part connection result of the human model is shown in Fig. 5d.

5.4 Hole Filling

(a)   **(b)**
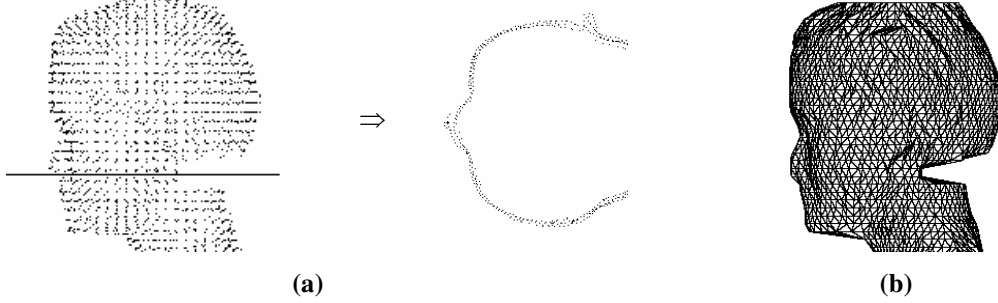
Fig. 15   Example hole and its horizontal intersection shape

While scanning a human model, some points may be missed (e.g., if the white swimming cap cannot cover the black hair, the points on the neck of the human model will always go missing – see Fig. 15a). Thus, after the mesh construction, there is still a cave on the surface (Fig. 15b). Here, we smooth such caves through minimizing the membrane energy of a mesh X

$$E_M(X) = \int X_u^2 + X_v^2 \tag{5}$$

which prefers functions with smaller surface area and the thin plate energy of X

$$E_{TP}(X) = \int X_{uu}^2 + 2X_{uv}^2 + X_{vv}^2 \tag{6}$$

which imposes strong bending. Their respective variational derivatives corresponds to the Laplacian and the second Laplacian:

$$L(X) = X_{uu} + X_{vv} \tag{7}$$

$$L^2(X) = X_{uuuu} + 2X_{uuvv} + X_{vvvv} \tag{8}$$

The variational calculus leads to simple characterizations of the corresponding minimum energy surface

$$L(X) = X_{uu} + X_{vv} = 0 \tag{9}$$

or

$$L^2(X) = X_{uuuu} + 2X_{uuvv} + X_{vvvv} = 0 \tag{10}$$

respectively. One common way to attenuate noise in a mesh is through a diffusion process

$$\frac{\partial X}{\partial t} = \lambda L(X) \tag{11}$$

where λ is a damping factor. By integrating equation (11) over time, a small disturbance will disperse rapidly in its neighborhood, smoothing the high frequencies, while the major shape will only be slightly degraded.

The Laplacian operators (7) and (8) can be linearly approximated at each vertex by the umbrella operator [17, 18]. To construct the operator, we have to choose an appropriate parameterization in the vicinity of each vertex. The umbrella-algorithm is derived by choosing a symmetric parameterization [19]

$$(u_i, v_i) = \left(\cos(2\pi \frac{i}{n}), \sin(2\pi \frac{i}{n}) \right), \quad i = 0, \ldots, n-1 \tag{12}$$

with n being the valence of the center vertex p.

With the special parameterization (equation (12)), the discrete representation of the Laplacian $L(X)$ turns out to be the umbrella operator

$$u(p) = \frac{1}{n} \sum_{i=0}^{n-1} (p_i - p) \tag{13}$$

with p_i being the direct neighbors of p. The umbrella-operator can be applied recursively leading to

$$u^2(p) = \frac{1}{n} \sum_{i=0}^{n-1} (u(p_i) - u(p)) \tag{14}$$

as a discretization of $L^2(X)$.

The characteristic system for the corresponding unconstrained minimization problem have rows $u(p_i) = 0$ or $u^2(p_i) = 0$ respectively for the free vertices p_i. An iterative solving scheme approaches the optimal solution by solving each row of the system separately and cycling through the list of free vertices until a stable solution is reached. For the case of the membrane energy E_M, this leads to the local update rule

$$p_i \leftarrow p_i + u(p_i) \tag{15}$$

and for the thin plate energy E_{TP}, this leads to

$$p_i \leftarrow p_i - \frac{1}{v} u^2(p_i) \tag{16}$$

with $v = 1 + \frac{1}{n_i} \sum_j \frac{1}{n_{i,j}}$, where n_i and $n_{i,j}$ are the valences of the center vertex p_i and its j th neighbor respectively.

The minimization of the membrane energy always leads to more "flat" results, and the minimization of the thin plate energy always leads to more "bulgy" results [17]. Thus, while smoothing the area surrounded, we propose to first use $u(p)$ to "flat" the vertices with flag stored in the section 5.2 one by one. After that, we will iteratively apply $u^2(p)$ on those vertices to "bulge" the concave area. The final result is shown in Fig. 16.
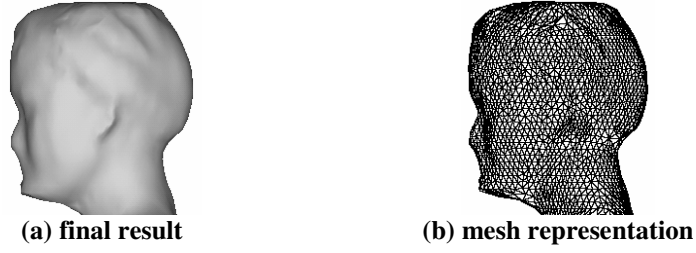
(a) final result   (b) mesh representation

Fig. 16   Final result of hole filling

6.   Semantic Feature Extraction

The objective of semantic feature extraction is to establish the correct correspondence between the constructed human model and domain-based applications. Here, we focus on the fashion industry domain. We should robustly extract a set of feature lines for a wide range of changes in body shape and size. To achieve this, we assume that each model stands approximately in a pre-specified pose; and fuzzy logic concept is applied to extract key features. Assistant features can be found from the key features by proportion rules used in the fashion industry [20, 21, 22]. There are five key features on a human model: armhole, crotch, neck, chest, and belly button. The armhole and crotch have already been extracted before constructing the mesh surface of a human model. Thus, in this section, we focus on how to extract the remaining three key features from a human model.
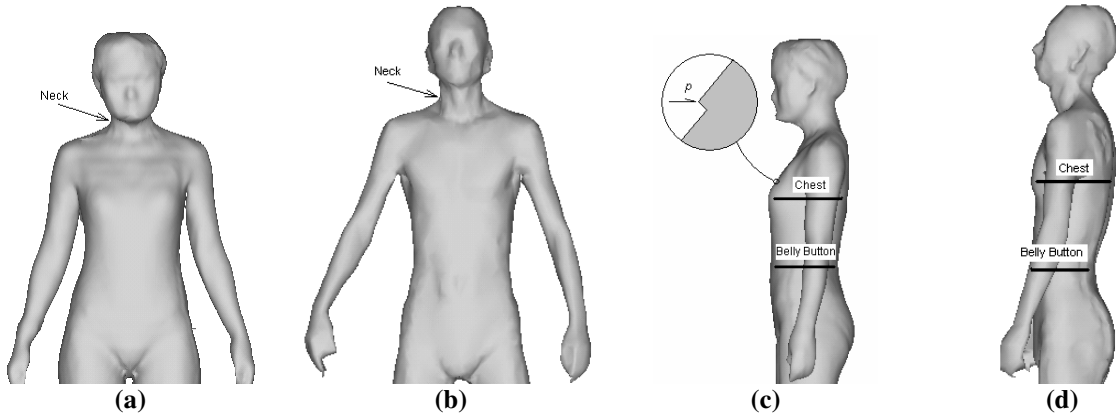

(a)   (b)   (c)   (d)

Fig. 17   Find neck, chest and belly button position

We extract the neck feature position through looking for extreme point around $\frac{7}{8}h_b$ of the human model from the silhouette of the front view; extract the chest feature position through looking for extreme point around $\frac{3}{4}h_b$ from the silhouette of the right view; and extract the belly button feature position around $\frac{5}{8}h_b$ of the human model from the silhouette of the right view (Fig. 17) (where h_b is the height of the human model). Our system expresses the recognition knowledge rules by condition statements (*if-then*). They are described below.

(If S is a horizontal cutting plane, $\lceil S \rceil$ represents a neighboring horizontal cutting plane above S, and $\lfloor S \rfloor$ represents a neighboring horizontal cutting plane below S.)

Rule 4: If there is a horizontal cutting plane S_{neck} at "about" $\frac{7}{8}h_b$ of the human model, S_{neck} is the neck plane when $Y_{\min}(S_{neck})$ is "smaller" than $Y_{\min}(\lfloor S_{neck} \rfloor)$, and $Y_{\min}(S_{neck})$ is "smaller" than or "equal" to $Y_{\min}(\lceil S_{neck} \rceil)$.

Rule 5: If there is a horizontal cutting plane S_{chest} at "about" $\frac{3}{4}h_b$ of the human model, S_{chest} is the chest plane when $X_{\max}(S_{chest})$ is "larger" than $X_{\max}(\lceil S_{chest} \rceil)$, and $X_{\max}(S_{chest})$ is "larger" than or "equal" to $X_{\max}(\lfloor S_{chest} \rfloor)$.

Rule 6: If there is a horizontal cutting plane S_{be} at "about" $\frac{5}{8}h_b$ of the human model, S_{be} is the belly button plane when $X_{\min}(S_{be})$ is "larger" than $X_{\min}(\lceil S_{be} \rceil)$, and $X_{\min}(S_{be})$ is "larger" than $X_{\min}(\lfloor S_{be} \rfloor)$.

In the rule 4, 5 and 6, the term "about" has the same meaning as the term "equal". Fuzzy logic concept is applied in the *if-then* statements to implement the rules. The fuzzy membership function for value comparison is shown in Fig. 18. Using the above fuzzy rules, we can efficiently extract the three key features; otherwise, an incorrect feature might be chosen (e.g., a system may believe the position p in Fig. 17b is the chest feature without using fuzzy logic).
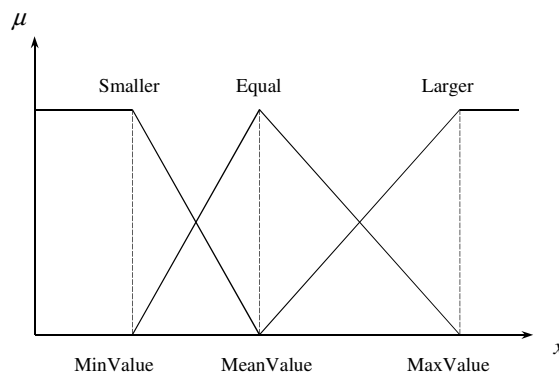

Fig. 18   Membership function of value comparison

After the five key features on a human model – armhole, crotch, neck, chest, and belly button, are extracted, other assistant features can be calculated by proportion rules used in the fashion industry [17, 18, 19]. This is very straightforward. The final feature human results for a female and a male are shown in Fig. 19. Such a

feature human model is the model to be stored in the 3D digital human model database. The statistics of the computational times are listed in Table 1. The whole procedure of building a model with 400,000 input points can be finished in one minute (include I/O).

Table 1 Statistics of computing

Model	Figure	Point Num	Time of Data Preparation (s)	Time of Mesh Construction (s)	Time of Feature Extraction (s)	Total Time (s)	Result
Female	19a	390,752	21.3	18.2	12.7	52.2	19b
Male	19c	366,874	20.1	19.5	13.3	52.9	19d

* The test is performed on a PIII 667 MHz PC with 256 MB RAM.

7. Applications of Feature Human Model

In this section we briefly talk about some applications that might benefit from this technology.

7.1 Dimensions Extraction

After a feature human is constructed, the dimensions of the human model can be obtained easily from the feature lines on the human model. Table 2 shows the dimensions of the female model and the male model in Fig. 19.
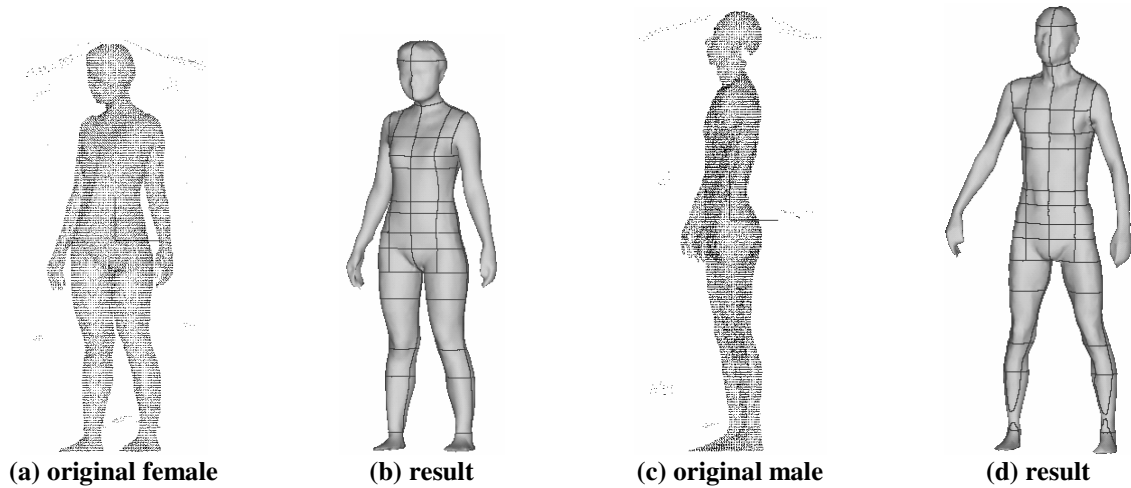

(a) original female　　**(b) result**　　**(c) original male**　　**(d) result**

Fig. 19　Results of feature human modeling

7.2 Parametric Design

The feature lines and feature points on the human model can be applied to the parametric design algorithm [23, 24] to deform the human model. For example, Fig. 20a shows the original feature human model; then we make it more chubby (shown in Fig. 20b); in the following, we scale the length of its leg and neck to make it longer (Fig. 20c); lastly, the shoulder slope of the human model is changed (result shown in Fig. 20d).

Table 2   Dimensions measurement result (unit: CM)

Dimensions	Female (Fig. 19b)	Male (Fig. 19d)
Height	162.92	175.67
Body Attitude (degree)	9.48	7.78
Head Height	22.71	24.29
C.B.Length	41.58	46.90
C.F.Length	39.58	44.90
Belly Button	95.82	100.79
Crotch Depth	22.71	24.29
In-Seam	73.11	76.50
Knee Length	39.39	41.28
Vertical Truck	145.87	156.28
Half Shoulder Width	19.92	20.90
Upper Arm Length	32.97	38.94
Lower Arm Length	26.87	28.98
Head Girth	63.08	61.95
Neck Girth	33.92	42.11
Shoulder Width	21.19	22.43
Cross Front	29.14	32.34
Cross Back	29.14	32.34
Chest	89.04	85.87
Lower Chest	85.46	79.09
Waist	71.50	68.87
Lower Waist	76.90	71.92
Hip/Seat	87.02	83.77
Lower Hip/Seat	96.02	90.28
Thigh Girth	59.91	53.61
Mid-thigh Girth	47.23	41.09
Knee Girth	37.36	32.40
Mid-calf Girth	37.16	33.32
Below-ankle Girth	23.55	23.96
Forearm Girth	76.18	24.21
Elbow Girth	25.01	23.72
Mid-lower-arm Girth	23.81	20.95
Wrist Girth	17.03	19.97

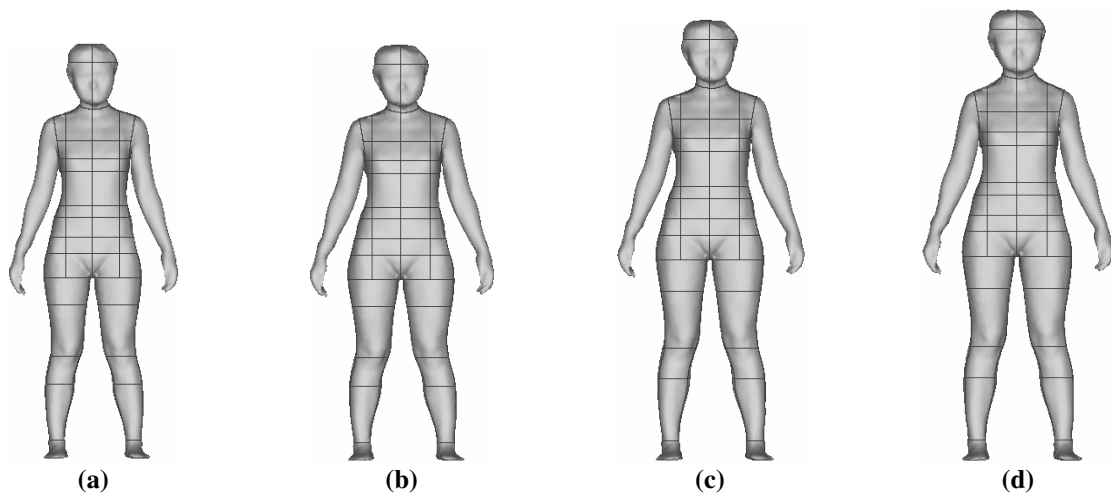(a)   (b)   (c)   (d)

Fig. 20   Example of human model parametric design

7.3 Three-dimensional Garment Construction

The technique described in this paper serves as the foundation of a new technique that allows pattern designers to design patterns directly on a 3D human model. Currently, the alternative technique just focuses on

the simulation of a 3D dressing result, but not on the 3D design. Thus, it needs the 2D patterns as the input. The demonstration of the new technique is shown in Fig. 21. This new technique gives pattern designers a tool to design patterns directly on the 3D human model according to the feature lines. For example, Fig. 21a shows the feature human model and the 3D garment profile given by designers (bold curves); variational subdivision scheme [15] is applied on the profile to construct a 3D surface to interpolate the profile (Fig. 21b); Fig. 21c and 21d are the draping results of a skirt. We found that the garment constructed by this new technique fit the human model nicely.
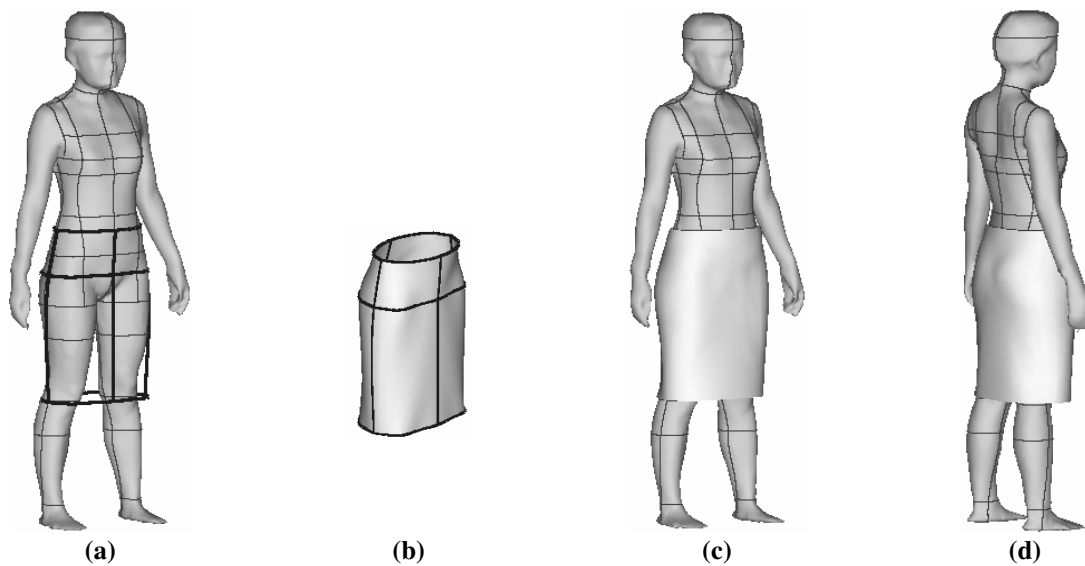

| (a) | (b) | (c) | (d) |

Fig. 21   Example of three-dimensional garment construction

8.   Conclusion and Discussion

This paper describes the development of a fuzzy logic concept based prototype system for constructing a feature human model to be stored in a 3D digital human model database by unorganized cloud points obtained from 3D laser scanners. This system is implemented on Windows NT, using Visual C++ and OpenGL Library. The whole procedure consists of three steps: in step 1, noisy points are removed, and the orientation of the human model is adjusted; in step 2, a feature based mesh generation algorithm is applied on the cloud points to construct the mesh surface of the human model; in step 3, semantic features of the human model are extracted from the mesh surface. The result shows that the fuzzy logic based system can capture the key features of the human model satisfactorily. Compared with earlier approach, our method has the following advantages:

- The topology of the human model is strongly preserved (benefit by the approach of features).
- The algorithm is highly efficient for using feature approach (the whole procedure is complated in one minute with about 400,000 input points).
- The robustness of our system is improved by applying fuzzy logic concept.

- More details can be constructed than the surface approximation approaches.

At the end of the paper, in order to demonstrate the functionality of the feature human model, potential applications of feature human models are given.

For noise filtering, our rules can only delete noisy points that are "far" from the surface of the human model. However, in practice we find that sometimes the noisy points are "close" to the surface of the model. More complex knowledge rules should be defined to deal with this problem. While extracting key features from the human model, the fuzzy rules may fail in some special cases. We simply use the default positions ($\frac{7}{8}h_b$, $\frac{3}{4}h_b$ or $\frac{5}{8}h_b$) to deal with the special cases.

Acknowledgement

References

[1]   Fischer A., and Park S., Remote sensing and LOD modeling for manufacturing products. International Journal of Advanced Manufacturing and Technology, pp. 91-94, 1998.

[2]   Varady T., Martin R. R., and Cox J., Reverse engineering of geometry models – an introduction. Computer Aided Design, 1997, 29(4): 255-268.

[3]   Au C.K., and Yuen M.M.F., Feature-based reserve engineering of mannequin for garment design. Computer Aided Design, 1999, 31(12): 751-759.

[4]   Hoppe H., DeRose T., Duchamp T., Halstead M., Jin H., McDonald J., Schweitzer J., and Stuetzle W., Piecewise smooth surface reconstruction. SIGGRAPH 94 Conference Proceedings, 1994, pp.295-302.

[5]   Ko. H., Kim M.S., Park H.G., and Kim S.W., Face sculpturing robot with recognition capability. Computer Aided Design, 1994, 26(11): 814-821.

[6]   Ma W., and He P., B-spline surface local updating with unorganised points. Computer Aided Design, 1998, 30(11): 853-862.

[7]   Barhak J., and Fischer A., Parameterization for reconstruction of 3D freeform objects from laser-scanned data based on a PDE method. The Visual Computer, vol. 17, no. 6, 2001, pp.353-369.

[8]   Sienz J., Szarvasy I., Hinton E., and Andrade M.L., Computational modelling of 3D objects by using

        fitting techniques and subsequent mesh generation. Computers & Structures, vol.78, no.1-3, 2000,

        pp.397-413. Publisher: Elsevier, UK.

[9]   Doncescu A., Organized mesh design applied in the body simulation. Inst. Comput. Sci. Machine

        Graphics & Vision, vol.9, no.1-2, 2000, pp.93-102, Poland. (6th Conference on Computer Graphics and

        Image Processing, GKPO'2000, Podlesice, Poland, 15-19 May 2000)

[10]   Rodriguez A., Espadero J.M., Lopez D., and Pastor L., Delaunay surface reconstruction from scattered

        points. Discrete Geometry for Computer Imagery 9th International Conference, DGCI 2000. Proceedings

        (Lecture Notes in Computer Science Vol.1953). Springer-Verlag. 2000, pp.272-283. Berlin, Germany.

[11]   Dobson G.T., Waggenspack Jr. W.N., and Lamousin H.J., Feature based models for anatomical data

        fitting. Computer Aided Design, 1995, 27(2): 139-146.

[12]   Marchand-Maillet S., and Sharaiha Y.M., Binary digital image processing: a discrete approach. San

        Diego, Calif.; London: Academic, 2000.

[13]   Chen P.C.L., and Xie S., Freehand drawing system using a fuzzy logic concept. Computer Aided Design,

        1996, 28(2): 77-89.

[14]   Meyers D., Skinner S., and Sloan K., Surface from Contours. ACM Transaction on Graphics, vol. 11, no.

        3, 1992, pp. 228-258.

[15]   Keppel E., Approximating complex surfaces by triangulation of contour lines. IBM Journal Res. Develop,

        Jan. 1975, pp. 2-10.

[16]   Ekoule A.B., Peyrin F.C., and Odet C.L., A triangulation algorithm from arbitrary shaped multiple planar

        contours. ACM Transaction on Graphics, vol. 10, no. 2, 1991, pp. 182-199.

[17]   Kobbelt L., Campagna S., Vorsatz J., and Seidel H.P., Interactive multi-resolution modeling on arbitrary

        meshes. SIGGRAPH 98 Conference Proceedings. ACM., 1998, pp.105-114. New York, NY, USA

[18]   Kobbelt L., Discrete fairing and variational subdivision for freeform surface design. The Visual

        Computer, vol.16, no.3-4, 2000, pp.142-158. Publisher: Springer-Verlag, Germany.

[19]   Kobbelt L., Discrete Fairing. Proceeding of the Seventh IMA Conference on the Mathematics of

        Surfaces' 97, 1997, pp.101-131.

[20]   Solinger J., Apparel manufacturing handbook: analysis, principles, and practice. Publisher: Columbia,

        S.C.: Bobbin Media Corp., 1988.

[21]   Taylor P.J., and Shoben M.M., Grading for the fashion industry: the theory and practice. Publisher: Cheltenham, England Thornes, 1990.

[22]   Cooklin G., Pattern grading for women's clothes: the technology of sizing. Publisher: Oxford : BSP Professional Books, 1990.

[23]   Lee A.W.F., Sweldens W., Schroder P., Cowsar L., and Dobkin D., MAPS: multiresolution adaptive parameterization of surface. SIGGRAPH 98 Conference Proceedings. ACM. 1998, pp.95-104. NewYork, NY, USA.

[24]   Praun E., Sweldens W., and Schroder P., Consistent mesh parameterizations. SIGGRAPH 2001 Conference Proceedings, 2001. ACM. NewYork, NY, USA.